



ELSEVIER

Contents lists available at ScienceDirect

Journal of Luminescence

journal homepage: [www.elsevier.com/locate/jlumin](http://www.elsevier.com/locate/jlumin)

# Tunnel conduction regimes, white-light emission and band diagram of porous silicon–zinc oxide nanocomposites



D. Gallach-Pérez<sup>a</sup>, A. Muñoz-Noval<sup>b</sup>, L. García-Pelayo<sup>a</sup>, M. Manso-Silván<sup>a,\*</sup>,  
V. Torres-Costa<sup>a,c</sup>

<sup>a</sup> Departamento de Física Aplicada and Instituto de Ciencia de Materiales Nicolas Cabrera, Universidad Autónoma de Madrid, Campus de Cantoblanco, 28049 Madrid, Spain

<sup>b</sup> Department of Applied Chemistry, Hiroshima University, Hiroshima 739-852, Japan

<sup>c</sup> Centro de Micro-Análisis de Materiales, Universidad autónoma de Madrid, Campus de Cantoblanco, 28049 Madrid, Spain

## ARTICLE INFO

### Article history:

Received 1 July 2016

Received in revised form

20 October 2016

Accepted 21 October 2016

Available online 28 October 2016

### Keywords:

Porous silicon

Zinc oxide

Electroluminescence

White light

Light-emitting devices

## ABSTRACT

Porous-Silicon/Zinc Oxide (PS-ZnO) nanocomposites can be processed by a combination of electrochemical etching of PS and sol-gel infiltration of ZnO, which leads to complex interfaces of ZnO permeated in the PS matrix. In this work, an approach consisting on the determination of transport mechanisms and identification of electroluminescence emission bands from the heterojunction, has been followed to derive the energy band diagram. Charge transport at room temperature has been determined in ITO/PS-ZnO/p<sup>+</sup>-Si/Al structures through current-voltage characteristics, showing that direct and Fowler-Nordheim (FN) tunneling are the main conduction mechanisms at low and high bias voltages, respectively. White electroluminescence composed of three main bands (~490, ~550 and ~620 nm) is observed at forward bias. Emission starts at a threshold voltage of  $3.9 \pm 0.2$  V, in coincidence with the change in conduction mechanism from direct to FN tunneling. A band diagram of the device is derived from the emission and transport properties, which is coherent with previous electronic and microstructural properties of the starting n-ZnO and p<sup>+</sup>-Si.

© 2016 Elsevier B.V. All rights reserved.

## 1. Introduction

Composites based on functional nanomaterials hosted within matrices of different nature are promising structures for light-emitting devices. Such nanocomposites can consist of a wide range of compounds including all inorganic [1], all organic [2,3] and hybrid structures [4–6]. The advanced functionality of the proposed structures contrasts with the little knowledge on fundamental aspects such as their electronic properties (charge transport mechanisms and associated energy band diagrams). First approaches to face this challenge would be welcome, especially from purely inorganic systems, counting with already well characterized semiconductor phases in the bulk and the nanoscale.

In particular, porous silicon (PS) has attracted much attention since the discovery of its efficient luminescence at room temperature (RT) [7], which makes this material especially attractive for Si-based optoelectronic applications. Indeed, shortly after such discovery, the first PS-based light-emitting device was reported [8]. The PS permeable matrix allows the integration of a wide

range of materials that have been studied as potential light emitters [9–11]. A particular approach consists in filling the PS pores with transparent conductive materials [9]. Following this idea, the combination of PS and ZnO led in a first stage to the processing of white photoluminescent composites [12–15] and, later on, to the fabrication of solid-state white-light sources (SSWLS) based on layered composites [13,16]. Indeed, this approach allows combining the optoelectronic properties of PS and ZnO, while at the same time, establishes a way to integrate ZnO with Si-based IC technology [17,18].

Noteworthy, PS and ZnO constitute an ideal couple of well characterized materials. On the one hand, PS exhibits strong efficient red-orange luminescence at RT caused by a Si band-gap expansion [19]. Exciton confinement is induced in Si quantum dots (QDs) formed during the electrochemical etching process of mesoporous Si [7]. The shape, size distribution and lattice parameters of these Si QDs naturally embedded in PS have been successfully studied earlier by transmission electron microscopy [20,21]. In addition, QDs remain inside a porous matrix passivated by silica with a high surface to volume ratio [22], which optimizes their optical coupling.

On the other hand, ZnO is a wide band gap semiconductor

\* Corresponding author.

E-mail address: [dario.gallach@uam.es](mailto:dario.gallach@uam.es) (D. Gallach-Pérez).

( $E_{g,ZnO} = 3.37$  eV at RT) with a high exciton binding energy (60 meV). This material has a characteristic photoluminescence composed of a strong UV emission as a result of band-to-band exciton recombinations and a blue-green emission due to the presence of available states in the bandgap caused by intrinsic defects. In fact, some of these intrinsic defects, such as oxygen vacancies [23] and carbon substitution of the cation [24] confer ZnO an n-type character.

EL from PS was previously measured using ZnO as transparent conductive front-side contact [16], and a Fowler-Nordheim transport mechanism was observed in agreement with previous reports on PS [25]. In other works, white EL is achieved in PS-ZnO:In structures formed by sputtering [11]. However, the microstructural details do not allow defining the formation of a permeated nanocomposite and amorphous interface phases are rather described.

The objective of the present work is to produce PS-ZnO SSWLS devices, ensuring the presence of an infiltrated ZnO with no additional doping into the anodized PS matrix [9]. We aim at retrieving from current-voltage (J-V) characteristics and EL spectra an energy band diagram of the formed heterojunction. The development of such band diagram to explain the processes that occur in the structure may be useful to improve its practical properties as well as serve as basement for understanding similar composite materials.

## 2. Experimental

The device is prepared by using PS substrates formed by the electrochemical anodization of  $p^+$ -type (B-doped), low-resistivity ( $0.01 < \rho < 0.02 \Omega \cdot \text{cm}$ ), (100) Si wafers in a HF(48wt):EtOH solution (1:2). The electrochemical process is carried out at RT, applying a constant current density of  $120 \text{ mA} \cdot \text{cm}^{-2}$  for 90 s resulting in  $1.1 \pm 0.1 \mu\text{m}$  thick mesoporous columnar structures (i.e. compatible for permeation and exhibiting photoluminescence) [26]. Before the etching, an Al ohmic contact is deposited by electron-beam evaporation on the backside of the wafer.

The sol-gel technique has been described to produce proper composites with adjustable optoelectronic properties (i.e. light emission) since low surface tension ZnO precursors are able to permeate PS with precise  $\text{Zn}^{2+}$  concentrations [27,28]. Thus, the PS-ZnO nanocomposites were synthesized after PS permeation with a 0.2 M sol of zinc acetate dihydrate ( $\text{Zn}(\text{CH}_3\text{COO})_2 \cdot 2(\text{H}_2\text{O})$ ,  $\geq 98\%$ ) diluted in absolute ethanol and monoethanolamine (MEA,  $\text{C}_2\text{H}_7\text{NO}$ , with  $[\text{MEA}] = [\text{Zn}^{2+}]$ ). After sol aging, 50  $\mu\text{L}$  are deposited by spin-coating at 2.5 krpm during 30 s over the PS substrates. After RT condensation, the composites were pre-annealed at  $200^\circ\text{C}$  for 5 min. to remove hydrocarbon byproducts. Coating steps are repeated 20 times before annealing the structure one hour at  $600^\circ\text{C}$  to obtain the final PS-ZnO nanocomposites. The device is completed by depositing a front transparent indium tin oxide (ITO) contact by electron beam evaporation.

Sample thickness and morphology were studied by electron microscopy using a Philips XL-40 FEG Field-Emission Scanning Electron Microscope (FESEM). J-V characteristics were measured by forward-biasing the device at 10 V to measure the EL spectra between 300 nm and 800 nm using the photomultiplier detector polarized at 250 V from an Aminco Bowman series 2 luminescence spectrometer.

## 3. Results

The FESEM image in Fig. 1(a) shows the surface of the PS-ZnO nanocomposite, allowing to infer an underlying porous structure

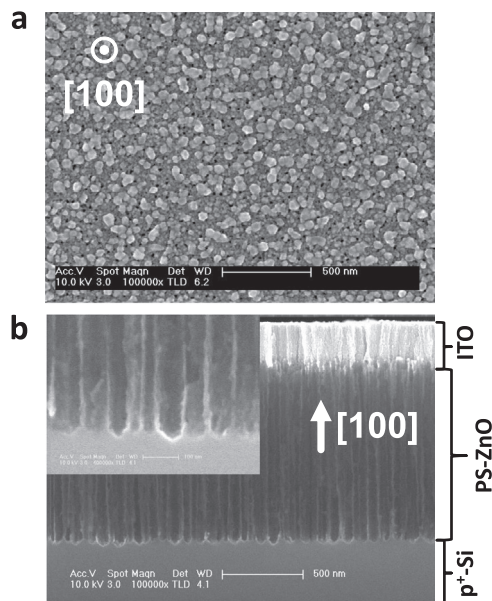


**Fig. 1.** (a) Top view of the sample before the ITO contact deposition. (b) Cross-section of the full ITO/PS-ZnO/ $p^+$ -Si structure. Inset: detailed view from the bottom of the pores.

with an ad-layer of nucleated structures. This evidences a distribution of ZnO crystals (mean diameter  $75 \pm 20$  nm) covering 55% of the surface as determined by using the ImageJ software [29]. The formation of these surface nanocrystals is promoted by the pore inhomogeneities, which spread isolated nucleation centers along the surface. Fig. 1(b) shows a cross-section of the nanocomposite junction after ITO contact processing (i.e. ITO/PS-ZnO/ $p^+$ -Si). The image reveals that PS pores propagate during etching along the [100] direction as expected for highly-doped  $p^+$ -type (100) Si [30]. In addition, the inset shows a detail of the  $p^+$ -Si/PS-ZnO interface in which a diffuse ZnO can be observed permeating some of the pores, forming a delocalized interface, as previously supported by microscopic and spectroscopic data (Rutherford Backscattering Spectroscopy) [31].

The experimental setup used to test the device is shown on Fig. 2(a), which is forward biased when the probe is set at negative voltages with respect to the back contact. Fig. 2(b-e), reveal that white EL is observed when the structure is forward biased at voltages above  $V_{FB} > 4$  V. The light is emitted at localized spots over the surface, which can be explained by the incomplete PS surface coverage.

The EL spectrum was acquired at  $V_{FB} = 10$  V forward bias (Fig. 2(f)), value ca. 20% below the maximum voltage that the structure is capable to withstand. The spectrum can be resolved in three main emission bands labeled as A, B and C. Band A is centered at 625 nm (1.98 eV), corresponding to a visible orange-red emission produced by quantum confined exciton recombination in PS QDs [32]. The band width (ca. 500- 750 nm) is related to the Si QDs size distribution [20,21]. Applying theoretical models developed for small semiconductor crystallites [33], refined for indirect band-gap semiconductor QDs [34], a Si QDs size of  $20 \pm 3 \text{ \AA}$  has been indirectly measured.

Bands B and C are centered at 550 nm (2.25 eV) and 490 nm (2.54 eV), respectively. Both are related to electronic transitions between the ZnO conduction band (CB) and deep level native point defects in its crystalline structure. However, silica formed at the PS surface after the thermal annealing may partially contribute to the 490 nm emission. These bands show a broadening, which can be related to the local structure of the intrinsic defects affecting the energy levels in the gap. It is known that the annealing

Download English Version:

<https://daneshyari.com/en/article/5397464>

Download Persian Version:

<https://daneshyari.com/article/5397464>

[Daneshyari.com](https://daneshyari.com)